Optical measurement of size and complex index of laser-damage precursors: the inverse problem

Laurent Gallais, Philippe Voarino, and Claude Amra

Institut Fresnel (Unité Mixte de Recherche, Centre National de la Recherche Scientifique), Ecole Nationale Supérieure de Physique de Marseille, Domaine Universitaire de St Jérôme 13397, Marseille Cedex 20, France

Received July 24, 2003; revised manuscript received July 24, 2003; accepted December 10, 2003

An indirect optical method for determining size and complex refractive index of laser-damage precursors in optical materials is presented. The method is described in detail, with special attention to all assumptions. Results are given for a series of thin-film SiO_2 layers. © 2004 Optical Society of America

OCIS codes: 140.3330, 160.6030, 310.0310.

1. INTRODUCTION

Much has been said about laser-induced damage in optical materials, which remains today a key limitation for optics involving high-energy densities. Although it is now admitted that nanocenters or precursors are at the origin of low damage thresholds in optical coatings and substrates,[1–10] little progress in improving the laser-damage threshold has been observed in the last few years, in spite of laser conditioning[11–23] for specific materials and sophisticated vacuum deposition technologies.[24–26] This situation is surely the result of a lack of detectivity in the characterization techniques of such coatings and substrates because the density and the threshold of precursors are the only information that can be extracted from damage-probability curves.[9,27–30] Obviously the size and complex index of a precursor should be key data to help us in the localization, detection, and identification of defects and would permit feedback of the production technology of microcomponents and substrates. However, such characterization cannot be made at this time for at least two main reasons:

- First, the density of precursors is very low in the bulk of materials, of the order of a few defects in a cube with a 100-μm side.[9,31] This low density makes the localization of defects with nonoptical techniques difficult, so the physicochemical properties of precursors remain unknown. At surfaces the precursor densities are much higher[9,31] (by several orders of magnitude) but are still not known, probably because of a lack of sensitivity or detectivity in the characterization techniques.
- Second, the precursors are rather small, and their indices can be close to the average index of the surrounding material, so absorption and scattering from isolated precursors remain below the detectivity of modern optical techniques such as photothermal microscopy[32–34] and ellipsometry of angle-resolved scattering.[35]

It should be noted here that all precursors under study must be discriminated from visible defects, such as pits or scratches, that can be revealed by different kinds of optical microscopy (Nomarsky, dark-field, total internal reflection,[36,37] ...). In the bulk of fused silica, for instance, nondestructive optical techniques reveal a perfectly homogeneous medium, although we know that precursors are present and create damage under laser irradiation. The situation is analogous at surfaces, provided that damage experiments are performed on high-quality samples or in regions free of visible defects, which is possible with laser beams of small spot sizes.[9,38] For these reasons we focused our efforts on the determination of size and complex index of precursors, using an indirect method based on the convergence of several optical data obtained from photothermal measurements and laser-damage probabilities. In this paper we present this alternative method and give results for single thin-film SiO_2 layers. Although special attention must be paid to all assumptions, the conclusions can be of great interest for the laser-damage community because knowledge of precursor size may allow adequate characterization techniques to be chosen for nondestructive detection. In addition, knowledge of a complex refractive index may facilitate investigations to identify the origin and nature of these precursors.

2. THRESHOLD AND DENSITY MEASUREMENTS OF LASER-DAMAGE PRECURSORS

In this section we explain how we measure laser-damage probability curves, denoted threshold curves, and extract the density of precursors. Results are given for a single SiO_2 layer.

A. Experimental Tools

The apparatus used at the Fresnel Institute for laser-damage experiments has been described in detail elsewhere,[9,38] and only a brief description is given here. The setup involves a single-mode YAG laser beam with 1.064-μm wavelength and 5-ns pulse duration (Fig. 1). The energy of the incident beam is measured with both a calorimeter and a pyroelectric detector. The beam profile of the focused beam is analyzed with an optical system linked to a CCD camera, and the temporal profile is measured with a fast photodiode. The sample is observed by

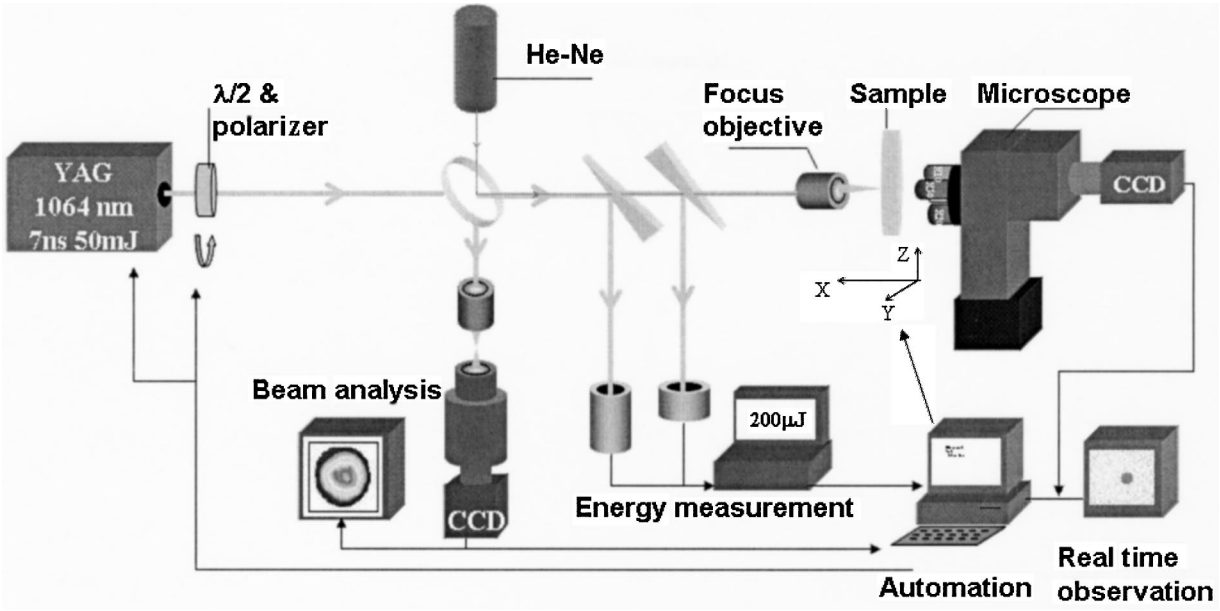

Fig. 1. Experimental setup for laser-damage testing.

an *in situ* optical microscope, which ensures real-time observation of the irradiated zone.

The whole apparatus is completely automatic and allows different damage test procedures [1-on-1,[39] *S*-on-1,[40] and *R*-on-1 (Ref. 41)] to be used. All sample translations, variable attenuations, laser shot synchronizations, and repetition rates are fully computer controlled. Also, the energy and the image of the focused beam are recorded for each shot. In addition, image processing has been implemented to produce accurate and real-time detection of damage.[38]

Using this apparatus, one can measure threshold curves in the bulk and at surfaces of optical components such as substrates, thin films, multilayers, and liquids. We recall that one obtains these curves by counting the number of damaged regions at each fluence F, which allows the probability of damage $P(F)$ to be estimated. Each curve $P(F)$ is plotted with 900 data points that involve 30 different fluences and 30 tested regions at each fluence. The shape and the slope of these curves are directly connected to the spot size and to the densities of precursors that are responsible for laser damage of dielectric materials,[2,4–6,9,27–29] as we demonstrate in Subsection 2.B.

B. Theoretical Tools

A phenomenological model was specifically developed to extract the precursor densities from the fit of the threshold curves and is used for 1-on-1 measurements[9,27–29] and for *S*-on-1 measurements.[30]

When precursors are assumed to be surface defects, the probability of damage can be expressed as a function of fluence F or energy density per unit of surface:

$$P(F) = 1 - \exp[-dS_T(F)], \tag{1}$$

where d is the surface density of defects and S_T is the region within the spot size where the energy density is greater than precursor threshold T. For a Gaussian beam, S_T is given by

$$S_T = \frac{1}{2} S \ln\left(\frac{F}{T}\right), \tag{2}$$

where S is the spot size defined when the energy is $1/e^2$ times its maximum value.

This model can be directly extended to bulk precursors[9,30] and consists in replacing effective surface $S_T(F)$ by effective volume $V_T(F)$. Notice that in all cases the precursor's density is assumed to be uniform. In addition, in thin films, surface and bulk models lead to identical results, provided that the following condition is fulfilled: $d = ed'$, where d and d' are the equivalent surface and bulk densities, respectively, and e is the film thickness.[31]

C. Results with Silica Thin Films

The samples under study are silica thin films deposited upon glass by a classic vacuum process. The average thickness of a sample is close to 1 μm. One of the threshold curves is plotted in Fig. 2 and reveals a low threshold of 19 J/cm^2 at 1.064 μm with 5-ns pulses. The curve can be approximated with probability formulas (1) and (2), which lead to a surface precursor density given by $d = 500/(100\,\mu\text{m})^2$. The corresponding bulk density

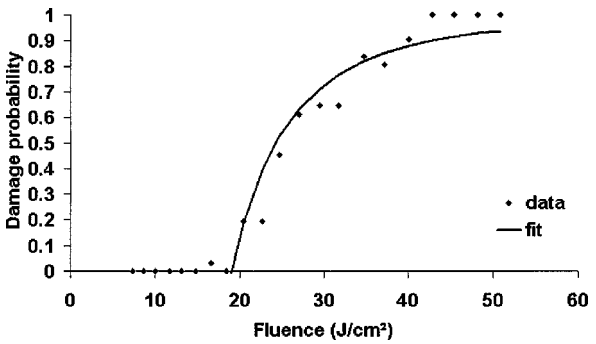

Fig. 2. Threshold curve of a silica thin film, together with fit of experimental data (λ = 1064 nm; beam diameter, 12 μm).

would be $d' = 5 \times 10^4/(100\,\mu\text{m})^3$. This density value is now used to extract the absorption of a single precursor. Note that here we do not consider the stationary field within the single layer because its average value is of the order of that of the incident field.

3. ABSORPTION EQUATION

Photothermal techniques allow low absorption in optical coatings to be measured down to 10^{-6}–10^{-8} times the incident power.[33,34] For the SiO_2 samples under study the absorption was measured with a 100-μm^2 pump beam at 1.064 μm,[32] and the result was close to $A = 5 \times 10^{-6}$.

As the surface density of precursors was found to be $d = 500/(100\,\mu\text{m})^2$, we assume that the measured absorption originates from the absorption of the precursor collection. Such an assumption is in agreement with several results[42–44] that revealed loss anomalies such as interface absorption and large root-mean-square absorption in optical samples. Therefore each precursor is assumed to absorb $A_p = A/d = 10^{-8}$ of the incident light, a value that we now relate to size and complex index of particles.

A. Calculation of Precursor Absorption

We consider a dielectric or metallic absorbing particle embedded in a transparent material such as silica. The density of monochromatic bulk absorption in the particle is given by the classic formula

$$\frac{\mathrm{d}A}{\mathrm{d}v} = \frac{\omega}{2}(\epsilon'' E^2 + \mu'' H^2), \tag{3}$$

where $\mathrm{d}v$ is a volume element, ϵ'' and μ'' are, respectively, the imaginary parts of the permittivity and the permeability of the precursor, ω is the temporal pulsation, and (E, H) is the electromagnetic field. We assume that the materials are nonmagnetic, such that absorption in a precursor is reduced to

$$\Delta A \approx \frac{\omega}{2}\epsilon'' \int_{\Delta v} E^2 \mathrm{d}v, \tag{4}$$

where Δv is the particle volume.

If we define the average field in the particle as

$$E_m^2 = \frac{1}{\Delta v}\int_{\Delta v} E^2 \mathrm{d}v, \tag{5}$$

the absorption of the precursor can be rewritten as

$$\Delta A = \frac{\omega}{2}\epsilon'' E_m^2 \Delta v. \tag{6}$$

Now we have to relate average field E_m to the incident optical power. In the case of weak beam divergence, incident surface power density $\mathrm{d}\Phi/\mathrm{d}S$ is connected to local incident electric field E_0 by

$$\frac{\mathrm{d}\Phi}{\mathrm{d}S} = \frac{k_s}{2\omega\mu_0}|E_0|^2, \tag{7}$$

where $k_s = 2\pi n_s/\lambda$, λ is the incident wavelength, n_s is the optical index of the surrounding material (silica in our case), and μ_0 is the permeability.

If we define a parameter β, taking into account interference and resonance effects on the particle, as

$$\beta = |E_m|^2/|E_0|^2, \tag{8}$$

the power density is rewritten as

$$\frac{\mathrm{d}\Phi}{\mathrm{d}S} = \frac{k_s}{2\omega\mu_0}\frac{|E_m|^2}{\beta}. \tag{9}$$

The formula for the precursor absorption is then turned into

$$\Delta A = \left(\frac{\omega^2\epsilon''\mu_0}{k_s}\right)\beta\Delta v\left(\frac{\mathrm{d}\Phi}{\mathrm{d}S}\right), \tag{10}$$

that is,

$$\Delta A = 4\pi\left(\frac{n'n''}{n_s}\right)\beta\left(\frac{\Delta v}{\lambda}\right)\left(\frac{\mathrm{d}\Phi}{\mathrm{d}S}\right). \tag{11}$$

Equation (11) permits one to calculate the power absorbed by a particle of volume Δv and complex index $n = n' + jn''$ under an irradiation $\mathrm{d}\Phi/\mathrm{d}S$ in a surrounding medium, n_s. It should be noted that parameter β may play a key role in the calculation because of potential overintensity within the precursor.

Let us establish an order of magnitude of these values. If we consider two classic cases in which 100 mW of power from a YAG laser ($\lambda = 1064$ nm) is focused on 100-μm^2 and 1-μm^2 surfaces, respectively, we obtain, for $n' \approx n_s$,

$$\Delta A \approx (n''\beta\Delta v) \times 10^{14}\ \text{W} \qquad (100\text{-}\mu\text{m}^2\ \text{surface}), \tag{12}$$

$$\Delta A \approx (n''\beta\Delta v) \times 10^{18}\ \text{W} \qquad (1\text{-}\mu\text{m}^2\ \text{surface}). \tag{13}$$

In Fig. 3 we show the absorbed power as a function of particle size (the precursor is assumed to be spherical) for the two irradiations, assuming a unit value of $n''\beta$. Consequently, effective values can be obtained by correction of the data of Fig. 3 with the appropriate extinction coefficient n'' of the particle and with parameter β that is calculated further.

Figure 3 can be of great interest for evaluation of the feasibility of precursor detection by means of photothermal techniques. For instance, we know that 10^{-7} is an

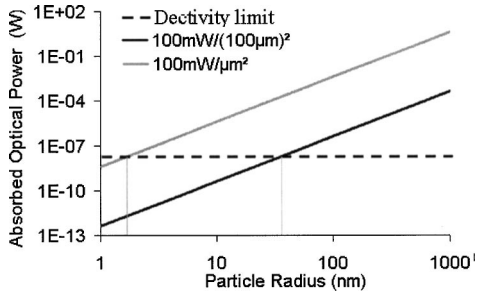

Fig. 3. Optical power absorbed by particles ($n' = n_s$ and $n''\beta = 1$) as a function of their radius. Irradiation is done with a 100-mW laser at 1064 nm, focused on a 100-μm^2 or a 1-μm^2 surface. Dashed line, average detectivity limit of photothermal measurements.

approximate limit value with which to quantify the detectivity of photothermal techniques[33,34] relative to absorption. With 100-mW beam power, such detectivity corresponds to an absorbed power of 10^{-8} W, as we have plotted in Fig. 3 (dashed line). Therefore this value can be compared with those shown by the two precursor absorption curves in the same figure. For example, an irradiation of 100 mW/(100 μm)^2 should permit the detection of absorption of precursors with radii greater than 30 nm. When the irradiation is increased to 100 mW/μm^2, precursors with 2-nm size could be detected. However, we must keep in mind that our results are obtained under the assumption that $n''\beta = 1$.

Now the E-field enhancement factor has been rigorously calculated as reported in various papers.[2,45–48] Such a factor depends on wavelength, particle size, and index, so parameter β has to be rigorously calculated in our conditions (nano to micronic particles embedded in silica and irradiated at 1064 nm).

B. Enhancement and Average Value of the Field within the Precursor

In relation (11), absorption ΔA is measured and incident flux $d\Phi/dS$ is known. If we could consider that the average field within the particle were close to the incident field, we would obtain $\beta = 1$, with the result that

$$\Delta A = 4\pi\left(\frac{n'n''}{n_s}\right)\left(\frac{\Delta v}{\lambda}\right)\left(\frac{d\Phi}{dS}\right). \tag{14}$$

Furthermore, if we assume that the real index of a particle is that of the surrounding medium ($n' = n_s$), relation (14) will be reduced to

$$\Delta A = 4\pi(n'')\left(\frac{\Delta v}{\lambda}\right)\left(\frac{d\Phi}{dS}\right). \tag{15}$$

Equation (15) will allow us to write a relationship between size and imaginary index of precursors in the form

$$n'' = g(R), \tag{16}$$

where R is the particle radius and $\Delta v = (4/3)\pi R^3$. Now we iterate the same reasoning without any approximation for parameter β. In this simulation we use Mie theory and calculate β as a function of all parameters, that is,

$$\beta = \beta(n', n'', R, \lambda). \tag{17}$$

A spherical particle of radius R and complex index $n = n' + jn''$ is assumed to be embedded in a surrounding transparent material of index $n_s = 1.52$ (glass) and illuminated with incident power density $d\Phi/dS$ at wavelength $\lambda = 1.064\ \mu$m. Mie calculation[49,50] allows all vector values of scattered field E_{sca} inside and outside the precursor to be found:

$$\mathbf{E}_{sca} = E_0 \sum_{n=1}^{N_{max}} i^n \frac{2n+1}{n(n+1)}[a_n^{sca}(R)\mathbf{m}_{o1n}^{(0)}(r, \theta, \varphi) - ib_n^{sca}(R)\mathbf{n}_{e1n}^{(0)}(r, \theta, \varphi)], \tag{18}$$

where E_0 is the E field's incident amplitude, N_{max} is the maximum order determined from Wiscombe's criteria's,[51] R is the sphere radius, a_n^{sca} and b_n^{sca} are coefficients determined with continuity relations, $\mathbf{m}_{o1n}^{(0)}$ and $\mathbf{n}_{e1n}^{(0)}$ are basis vectors, and r, θ, and φ are spherical coordinates.

Figure 4 shows the field in three directions inside and outside an absorbing particle ($n = 2 + j$). The local intensity-enhancement factor is strongly dependent of the particle size and complex index. To get an order of magnitude of this factor, we found maximum values near 10 for metallic particles ($n'' = 10$) with sizes of 1–100.

However, parameter β describes an average value, whereas relation (11) is given for the local field. To prevent integration of the local field inside the particle we use an integrated Mie formula that yields extinction Q_{ext} and scattering Q_{sca} cross sections of particles, that is,

$$Q_{sca} = \frac{2\pi}{k_s}\sum_{n=1}^{N_{max}}(2n+1)(|a_n^{sca}|^2 + |b_n^{sca}|^2), \tag{19}$$

$$Q_{ext} = \frac{2\pi}{k_s}\sum_{n=1}^{N_{max}}(2n+1)\mathrm{Re}(a_n^{sca} + b_n^{sca}). \tag{20}$$

Therefore absorption Q_{abs} of a single precursor can be calculated from Mie theory as

$$Q_{abs} = Q_{ext} - Q_{sca} = \Delta A/(d\Phi_0/dS), \tag{21}$$

$$\Rightarrow \Delta A = (Q_{ext} - Q_{sca})\Delta A/(d\Phi_0/dS). \tag{22}$$

At this step, with the measured value ΔA, we can obtain a relationship among the precursor parameters (n', n'', R). In Fig. 5 the curve $n'' = g(R) \pm \Delta n''(n')$ is calculated, with a range of values that is due to the uncertainty in real index n': $0.5 < n' < 5$. This range includes dielectric and metallic particles.

From these results it can be seen that, if the damage precursor is metallic ($n'' > 1$), its size will lie in the range 10–60 nm; if the particle is dielectric ($n'' < 10^{-3}$), however, its size will be greater than 200 nm.

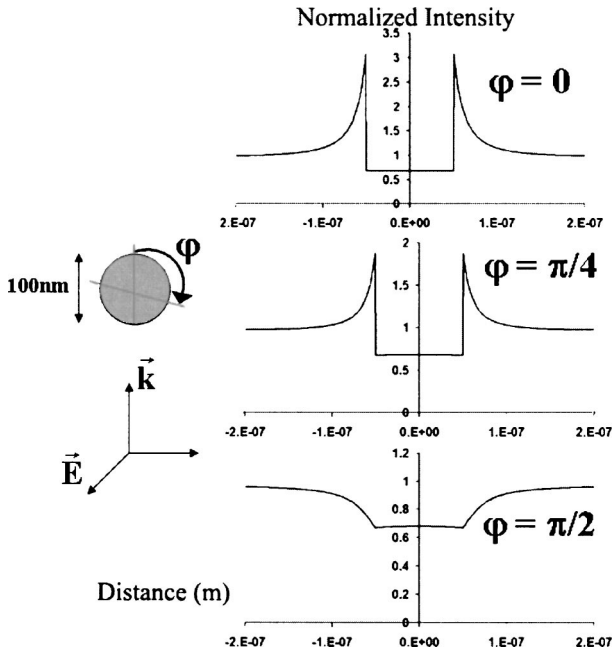

Fig. 4. E-field distribution inside and outside a 100-nm spherical particle of extinction index 1, irradiated at 1064 nm with polarization defined in this figure. The E-field distribution is represented for three polar angles in the incident plane.

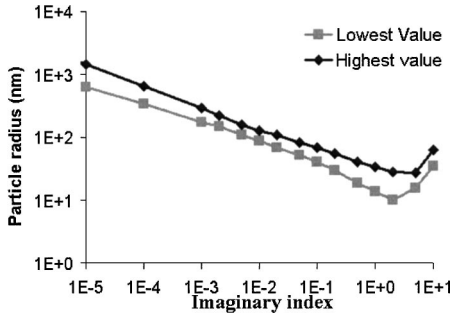

Fig. 5. Particle size as a function of extinction index, calculated from Eq. (11) for a SiO_2 film. Highest and lowest values are estimated from the uncertainty on n' ($0.5 < n' < 5$).

This result was obtained by measurement of the density and the absorption of precursors, coupled with the absorption equation. In Section 4 we show how this inverse problem can be completely solved by use of an additional threshold equation.

4. THRESHOLD EQUATION

As we have from Section 3 a first equation that links the imaginary index and size of precursors, we now use another property given by the threshold equation. For this we assume that the breakdown is reached when the maximum temperature within the particle exceeds the melting temperature T_m of the surrounding medium (glass).

We consider again an absorbing defect of radius R embedded in a homogenous material (silica) and irradiated by a plane wave with a Gaussian temporal profile (width at $1/e$, τ). Notation is given in Fig. 6. If we limit ourselves to unique heat transfer by conduction, the temperature is a function of ρ and t and follows the heat equation

$$\Delta T(\rho, t) - \frac{1}{a}\frac{\partial T(\rho, t)}{\partial t} = -\frac{S(\rho, t)}{b}, \tag{23}$$

where a and b are, respectively, the diffusivity and the conductivity of the different media. The term $S(\rho, t)$ is the source term (bulk density of absorption), which can be written as $S = S_0 \exp[-4(t^2/t^2)]$. $S_0 = dA/dv$ is obtained from Eq. (11). Considering the small size of the particle, we assume that this source term is spatially constant inside the sphere: $S_0 = \Delta A/\Delta v$. To solve Eq. (23) we consider the Fourier transform of the temperature:

$$T(\rho, t) \overset{\text{F.T.}}{\rightarrow} \hat{T}(\rho, \Omega). \tag{24}$$

Consequently the heat equation in the two media can be written as

$$\Delta \hat{T}_1(\rho, \Omega) + \alpha_1^2 \hat{T}_1 = -\frac{S_0}{2b_1}\sqrt{\pi}\tau \exp\left(-\frac{\pi^2}{4}\tau^2\Omega^2\right), \tag{25}$$

$$\Delta \hat{T}_2(\rho, \Omega) + \alpha_2^2 \hat{T}_2 = 0, \tag{26}$$

where $\alpha_i = (2\pi\Omega/2\alpha_i)^{1/2}(1 + j)$ and S_0 is the absorbed optical power defined above.

Applying the limit conditions, we can write the solutions to the two media as

$$\hat{T}_1(\rho, \Omega) = \frac{A_1}{\rho}\exp(j\alpha_1\rho) - \frac{A_1}{\rho}\exp(-j\alpha_1\rho) - \frac{S_0}{2\alpha_1^2 b_1}\sqrt{\pi}\tau \exp\left(-\frac{\pi^2}{4}\tau^2\Omega^2\right), \tag{27}$$

$$\hat{T}_2(\rho, \Omega) = \frac{A_2}{\rho}\exp(j\alpha_2\rho). \tag{28}$$

Solutions $\hat{T}_i$ are found by use of the boundary conditions. Temperatures T_i are then obtained by means of a numerical inverse Fourier transform:

$$T_i(\rho, t) = \text{F.T.}^{-1}[\hat{T}_i(\rho, \Omega)]. \tag{29}$$

We have applied this model of photoinduced temperature to an inclusion with a unit value of n'' (with 1 nm $< R < 1$ μm) embedded in silica with a unit value of n''. The particle is irradiated with an energy of 19 J/cm^2 at

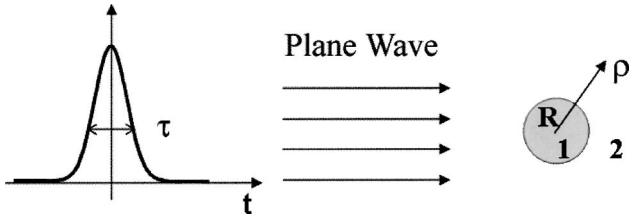

Fig. 6. Absorbing spherical particle (1) embedded in a homogenous non-absorbing medium (2) irradiated by a plane wave with a Gaussian temporal profile.

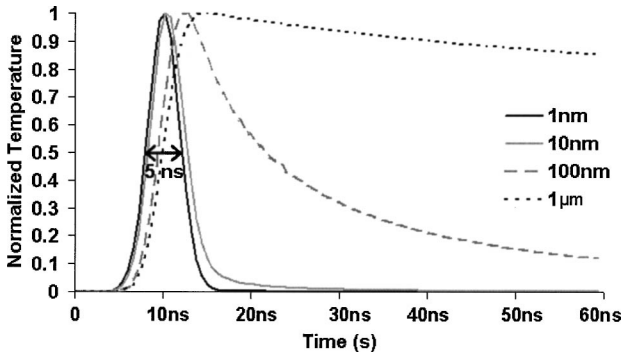

Fig. 7. Normalized temperature variations in particles embedded in silica of four diameters irradiated with an energy of 19 J/cm^2 at 1064 nm during 5 ns. $n''\beta = 1$.

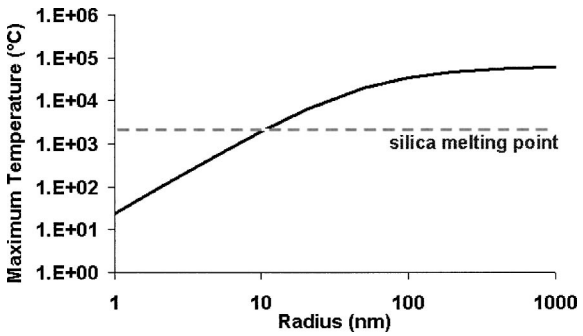

Fig. 8. Maximum temperature reached by particles embedded in silica and irradiated with an energy of 19 J/cm^2 at 1064 nm during 5 ns. Dashed line, temperature of the silica melting point (1883 °C). ($n''\beta = 1$.)

1064 nm at a pulse length of 5 ns, which corresponds to the threshold measured in silica layers in our test conditions (Section 2). First we consider thermal parameters that correspond to a metallic precursor, $a = 2.5 \times 10^{-5}\,\mathrm{m^2\,s^{-1}}$ and $b = 90\,\mathrm{W\,m^{-1}\,K^{-1}}$; and silica thermal parameters $a = 8.34 \times 10^{-7}\,\mathrm{m^2\,s^{-1}}$ and $b = 1.38\,\mathrm{W\,m^{-1}\,K^{-1}}$. Figure 7 illustrates the temperature variations at the particle–silica interface. These temperatures are normalized to permit their temporal responses to be compared as functions of precursor size. The maximum temperatures reached are shown in Fig. 8. These values are in good agreement with the results of Hopper and Uhlmann[1] for similar systems.

From these calculations it results that a metallic particle of radius >10 nm embedded in silica can initiate a damage process because the photoinduced temperature exceeds the melting point of silica irradiated at 19 J/cm^2 (Fig. 8). However, the precursors can also be dielectric and the same reasoning applied. Thus, if the melting of silica is considered a criterion of damage and because the source term in the heat equation depends on an extinction coefficient, the temperature prediction permits an estimation of particle size as a function of the imaginary index required for creation of damage in silica. The results are presented in Fig. 9. The range of value in this figure again reflects lack of knowledge of the real index but also lack of knowledge of the thermal coefficients (a_1 and b_1) of laser-damage precursors. We used $0.5 < n' < 5$, $1 \times 10^{-5}\,\mathrm{m^2\,s^{-1}} < a_1 < 1 \times 10^{-4}\,\mathrm{m^2\,s^{-1}}$ and $10\,\mathrm{W\,m^{-1}\,K^{-1}} < b_1 < 200\,\mathrm{W\,m^{-1}\,K^{-1}}$ (values taken from Ref. 52). Thus it is possible to take account of dielectric and metallic precursors, whatever the real index and thermal parameters.

Now it remains to use simultaneously the results of Figs. 5 and 9 to solve our problem.

5. DETERMINATION OF IMAGINARY INDEX AND SIZE OF LASER-DAMAGE PRECURSORS: THE INVERSE PROBLEM

At this step we obtained two relationships between size and complex index of precursors.

The first relation was found through the absorption equation and is written as

$$n'' = g(R) \pm \Delta n''(n'), \tag{30}$$

with an uncertainty in the real index n' that takes account of dielectric and metallic particles (Fig. 5).

The second equation was found through the threshold equation and is

$$n'' = h(R) \pm \Delta n''(n', a_1, b_1), \tag{31}$$

with an uncertainty in the thermal parameters (a_1, b_1) that takes account of dielectric and metallic particles (Fig. 9).

A combination of these data is presented in Fig. 10 and permits an evaluation of precursor parameters. The striped area in this figure indicates the domain where the precursors with absorption of 10^{-8} times the incident power induce damage in silica under 5-ns single-shot ir-

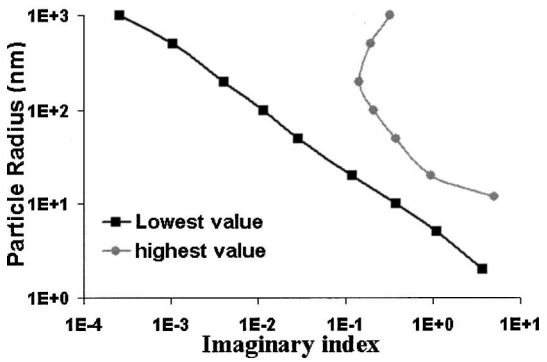

Fig. 9. Particle size as a function of extinction index, calculated from the modeling of Section 4. Highest and lowest values are estimated from the uncertainty on the different parameters (see text). Silica matrix.

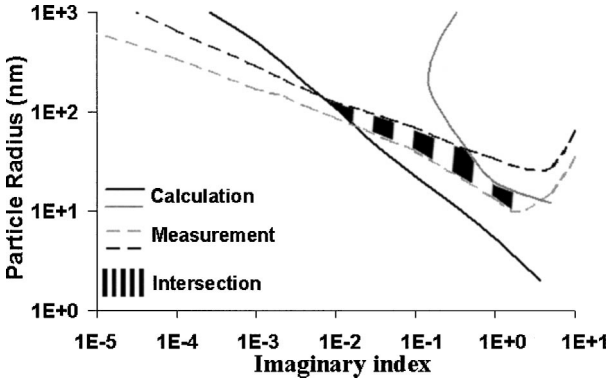

Fig. 10. Calculated and measured relationships between size and extinction index of the particle. Darker curves, lowest data; lighter curves, highest data. Striped area, intersection between thermal calculations and optical measurements, i.e., possible values of the radius and the extinction index of a laser-damage precursor embedded in silica.

radiation of 19 J/cm^2 at 1.064-μm wavelength. Therefore we conclude that the size range of precursors is

$$10\ \mathrm{nm} < R < 120\ \mathrm{nm} \tag{32}$$

and that the imaginary index lies in the range

$$9 \times 10^{-3} < n'' < 5. \tag{33}$$

Now, if we assume that the precursors are metallic, we obtain a particle radius close to 10 nm; dielectric precursors would give a particle radius close to 100 nm.

6. CONCLUSIONS

The size and the complex index of single-shot damage precursors were extracted by means of a specific procedure involving different data generated from threshold curves and photothermal measurements. For single thin films of SiO_2 we found a relationship between size and imaginary index of laser-damage precursors. These results will surely help in the physicochemical identification and current detection of defects. However, our procedure is valid under assumptions that we again clearly recall here:

- The precursors were assumed to be spherical and uniformly distributed, which permitted extraction of their surface density from the threshold curves.
- Low absorption in single SiO_2 thin films was assumed to be the result of absorption from the precursor

distribution, which allowed us to isolate absorption from a single precursor. The stationary field within the layer was not taken into account, but the enhancement field was calculated within the precursors.

- Damage was assumed to originate from an elevated temperature within the precursors, up to the fusion temperature of the surrounding medium.
- Finally, the photoinduced temperature from a 5-ns single-shot YAG laser was calculated under the assumption of unique heat conduction.
- Note that unknown real index and thermal parameter of precursors are responsible for errors in calculations and therefore for the limit of accuracy in characterization of damage precursors.

In a general way, to our knowledge this procedure is the first attempt at optical characterization of size and complex index of damage precursors. We expect this study to be systematically extended to the analysis of precursors in the bulk of substrates and within multilayers. The procedure should also allow threshold values to be predicted at different wavelengths and repetition rates. Finally, knowledge of the geometry and the complex index of precursors should soon assist in the application of adequate optical and nonoptical tools for further investigation. In all cases our results must now be checked with complementary techniques.

L. Gallais's e-mail address is laurent.gallais@fresnel.fr.

REFERENCES

1. R. W. Hopper and D. R. Uhlmann, "Mechanism of inclusion damage in laser glass," J. Appl. Phys. **41**, 4023–4037 (1970).
2. N. Bloembergen, "Roles of cracks, pores, and absorbing inclusions on laser induced damage threshold at surfaces of transparent dielectrics," Appl. Opt. **12**, 661–664 (1973).
3. M. R. Lange, J. K. McIver, and A. H. Guenther, "Pulsed laser damage in thin film coatings: fluorides and oxides," Thin Solid Films **125**, 143–155 (1985).
4. M. R. Kozlowski and R. Chow, "The role of defects in laser multilayer coatings," in *Laser-Induced Damage in Optical Materials: 1993*, H. E. Bennett, A. H. Guenther, M. R. Kozlowski, B. E. Newnam, and M. J. Soileau, eds., Proc. SPIE **2114**, 640–649 (1994).
5. J. Dijon, T. Poiroux, and C. Desrumaux, "Nanoabsorbing centers: a key point in laser damage of thin films," in *Laser-Induced Damage in Optical Materials: 1996*, H. E. Bennett, A. H. Guenther, M. R. Kozlowski, B. E. Newnam, and M. J. Soileau, eds., Proc. SPIE **2966**, 315–325 (1997).
6. H. Bercegol, "Statistical distribution of laser damage and spatial scaling law for a model with multiple defects cooperation in damage," in *Laser-Induced damage in Optical Materials: 1999*, G. J. Exarhos, A. H. Guenther, M. R. Kozlowski, K. L. Lewis, and M. J. Soileau, eds., Proc. SPIE **3902**, 339–346 (2000).
7. F. Y. Genin, A. Salleo, T. V. Pistor, and L. L. Chase, "Role of light intensification by cracks in optical breakdown on surfaces," J. Opt. Soc. Am. A **18**, 2607–2616 (2001).
8. S. Papernov and A. W. Schmid, "Correlations between embedded single gold nanoparticles in SiO_2 thin film and nanoscale crater formation induced by pulsed-laser radiation," J. Appl. Phys. **92**, 5720–5728 (2002).
9. J. Y. Natoli, L. Gallais, H. Akhouayri, and C. Amra, "Laser-induced damage of materials in bulk, thin film, and liquid forms," Appl. Opt. **41**, 3156–3166 (2002).
10. F. Bonneau, P. Combis, J. L. Rullier, J. Vierne, H. Ward, M. Pellin, M. Savina, M. Broyer, E. Cottancin, J. Tuaillon, M. Pellarin, L. Gallais, J. Y. Natoli, M. Perra, H. Bercegol, L. Lamaignre, M. Loiseau, and J. T. Donohue, "Study of UV laser interaction with gold nanoparticles embedded in silica," Appl. Phys. B **75**, 803–815 (2002).
11. P. A. Temple, W. H. Lowdermilk, and D. Milam, "Carbon dioxide laser polishing of fused silica surfaces for increased laser-damage resistance at 1064 nm," Appl. Opt. **21**, 3249–3255 (1982).
12. S. D. Allen, J. O. Porteus, and W. N. Faith, "Infrared laser-induced desorption of H_2O and hydrocarbons from optical surfaces," Appl. Phys. Lett. **41**, 215–218 (1982).
13. J. E. Swain, S. Stokowski, D. Milam, and G. Kennedy, "The effect of baking and pulsed laser irradiation on the damage threshold of potassium dihydrogen phosphate glass," Appl. Phys. Lett. **41**, 12–16 (1982).
14. M. E. Frink and J. W. Arenberg, "Temporary laser damage threshold enhancement by laser conditioning of antireflection-coated glass," Appl. Phys. Lett. **51**, 415–418 (1987).
15. M. R. Kozlowski, C. R. Wolfe, M. C. Staggs, and J. H. Campbell, "Large area laser conditioning of dielectric thin film mirrors," in *Laser-Induced Damage in Optical Materials: 1989*, H. E. Bennett, L. L. Chase, A. H. Guenther, B. E. Newnam, and M. J. Soileau, eds., Proc. SPIE **1438**, 376–390 (1990).
16. M. C. Staggs, M. Balooch, M. R. Kozlowski, and W. J. Siekhaus, "*In situ* atomic force microscopy of laser-conditioned and laser-damaged HfO_2/SiO_2 dielectric mirror coatings," in *Laser-Induced Damage in Optical Materials: 1991*, H. E. Bennett, L. L. Chase, A. H. Guenther, B. E. Newnam, and M. J. Soileau, eds., Proc. SPIE **1624**, 1–12 (1992).
17. C. R. Wolfe, M. R. Kozlowski, J. H. Campbell, M. Staggs, and F. Rainer, "Permanent laser conditioning of thin film optical materials," U.S. patent 5,472,748 (December 5, 1995).
18. E. Eva, K. Mann, N. Kaiser, B. Anton, R. Henking, D. Ristau, P. Weissbrodt, D. Mademann, L. Raupach, and E. Hacker, "Laser conditionning of LaF_3/MgF_2 dielectric coatings at 248 nm," Appl. Opt. **35**, 5613–5619 (1996).
19. M. Runkel, J. DeYoreo, W. Sell, and D. Milam, "Laser conditioning of KDP on the optical sciences laser using large area beam," in *Laser-Induced Damage in Optical Materials: 1997*, H. E. Bennett, A. H. Guenther, M. R. Kozlowski, B. E. Newnam, and M. J. Soileau, eds., Proc. SPIE **3244**, 51–63 (2001).
20. M. Staggs, M. Yan, and M. Runkel, "Laser raster conditioning of KDP and DKDP crystals using XeCl and Nd:YAG lasers," in *Laser-Induced Damage in Optical Materials: 2000*, G. J. Exarhos, A. H. Guenther, M. R. Kozlowski, K. L. Lewis, and M. J. Soileau, eds., Proc. SPIE **4347**, 400–407 (2001).
21. L. Lamaignère, M. Loiseau, H. Piombini, D. Plessis, and H. Bercegol, "Bulk damage and laser conditioning of KDP and DKDP crystals with Xe-F excimer light and the 3ω of a Nd:YAG laser," in *Laser-Induced Damage in Optical Materials: 2002*, G. J. Exarhos, A. H. Guenther, N. Kaiser, K. L. Lewis, M. J. Soileau, C. J. Stolz, A. Giesen, and H. Weber, eds., Proc. SPIE **4932**, 391–392 (2004).
22. J. A. Menapace, B. Penetrante, D. Golini, A. Slomba, P. E. Miller, T. Parham, M. Nichols, and J. Peterson, "Combined advanced finishing and UV-laser conditioning for producing UV-damage-resistant fused silica optics," in *Laser-Induced Damage in Optical Materials: 2001*, G. J. Exarhos, A. H. Guenther, K. L. Lewis, M. J. Soileau, and C. J. Stolz, eds., Proc. SPIE **4679**, 56–68 (2002).
23. J. E. Peterson, S. M. Maricle, R. M. Brusasco, and B. M. Penetrante, "Reduction of damage initiation density in fused silica optics via UV laser conditioning," U.S. patent 2002/0046579 (2002).
24. P. F. Gu and J. F. Tang, "Laser-induced damage resistance of thin-films polarizers prepared by ion-assisted deposition," Opt. Lett. **19**, 81–83 (1994).
25. J. Dijon, B. Rafin, C. Pellé, J. Hue, G. Ravel, and B. Andr, "100-J/cm^2 1.06 μm mirrors," in *Laser-Induced Damage in Optical Materials: 1999*, G. J. Exarhos, A. H. Guenther, M.

R. Kozlowski, K. L. Lewis, and M. J. Soileau, eds., Proc. SPIE **3902**, 158–168 (2000).
26. M. Alvisi, M. Di Giulio, S. G. Maronne, M. R. Perrone, M. L. Protopapa, A. Valentini, and L. Vasanelli, "HfO_2 films with high laser damage threshold," Thin Solid Films **358**, 250–258 (2000).
27. R. Picard, D. Milam, and R. Bradbury, "Statistical analysis of defect-caused damage in thin films," Appl. Opt. **16**, 1563–1571 (1977).
28. J. O. Porteus and S. C. Seitel, "Absolute onset of optical surface damage using distributed defect ensembles," Appl. Opt. **23**, 3796–3805 (1984).
29. R. M. O'Connell, "Onset threshold analysis of defect-driven surface and bulk laser damage," Appl. Opt. **31**, 4143–4153 (1992).
30. L. Gallais, J. Y. Natoli, and C. Amra, "Statistical study of single and multiple pulse laser-induced damage in glasses," Opt. Express **10**, 1465–1474 (2002), http://www.opticsexpress.org.
31. L. Gallais, "Laser damage in optical components—metrology, statistical and photo-induced analysis of precursor centers," Ph.D. dissertation (Université d' Aix-Marseille III, France, 2002).
32. M. Commandré and P. Roche, "Characterization of optical coatings by photothermal deflection," Appl. Opt. **34**, 5021–5034 (1996).
33. A. During, "Photothermal microscopy and laser damage," Ph.D. dissertation (Université d' Aix-Marseille III, France, 2002).
34. A. During, C. Fossati, and M. Commandré, "Multiwavelength imaging of defects in ultraviolet optical materials," Appl. Opt. **41**, 3118–3126 (2002).
35. C. Deumié, H. Giovannini, and C. Amra, "Angle-resolved ellipsometry of light scattering: discrimination of surface and bulk effects in substrates and optical coatings," Appl. Opt. **41**, 3362–3369 (2002).
36. P. A. Temple, "Total internal reflection microscopy: a surface inspection technique," Appl. Opt. **20**, 2656–2664 (1981).
37. L. Sheehan, M. R. Kozlowski, and D. Camp, "Application of total internal reflection microscopy for laser damage studies on fused silica," in *Laser-Induced Damage in Optical Materials: 1997*, H. E. Bennett, A. H. Guenther, M. R. Kozlowski, B. E. Newnam, and M. J. Soileau, eds., Proc. SPIE **2714**, 282–295 (1998).
38. L. Gallais and J. Y. Natoli, "Optimized metrology for laser damage measurement—application to multiparameter study," Appl. Opt. **42**, 960–971 (2003).
39. International Organization for Standardization, "Determination of laser-damage threshold of optical surfaces. 1. 1-on-1 test," standard ISO 11254-1 (International Organization for Standardization, Geneva, 2000).
40. International Organization for Standardization, "Determination of laser-damage threshold of optical surfaces. 2. *S*-on-1 test," standard ISO 11254-2 (International Organization for Standardization, Geneva, 2001).
41. J. Hue, P. Garrec, J. Dijon, and P. Lyan, "*R*-on-1 automatic mapping: a new tool for laser damage testing," in *Laser-Induced Damage in Optical Materials: 1995*, A. H. Guenther, M. R. Kozlowski, B. E. Newnam, and M. J. Soileau, eds., Proc. SPIE **2714**, 90–101 (1996).
42. A. Gatto and M. Commandré, "Multiscale mapping technique for the simultaneous estimation of absorption and partial scattering in optical coatings," Appl. Opt. **41**, 225–234 (2002).
43. M. Ranier, P. Volto, G. Albrand, J. Y. Natoli, C. Amra, B. Pinot, and B. Geenen, "Waveguide losses by photothermal techniques in multilayers for laser damage investigation," in *Laser-Induced Damage in Optical Materials: 1997*, H. E. Bennett, A. H. Guenther, M. R. Kozlowski, B. E. Newnam, and M. J. Soileau, eds., Proc. SPIE **3244**, 484–490 (1998).
44. L. Escoubas, A. Gatto, G. Albrand, P. Roche, and M. Commandré, "Solarization of glass substrates during thin-film deposition," Appl. Opt. **37**, 1883–1889 (1998).
45. P. Temple and M. J. Soileau, "Resonant defect enhancement of the laser electric field," in *Damage in laser materials: 1976*, A. J. Glass and H. E. Bennett, eds., Nat. Bur. Stand. (U.S.) Spec. Publ. **462**, 371–378 (1976).
46. M. R. Kozlowski, J. F. DeFord, and M. C. Staggs, "Laser-damage susceptibility of nodular defects in dielectric mirror coatings: AFM measurements and electric-field modeling," AIP Conf. Proc. **288**, 44–49 (1993).
47. K. F. Ferris, G. J. Exarhos, and S. M. Riser, "Enhancement factors for local electric fields in inhomogeneous media," in *Laser-Induced Damage in Optical Materials: 1994*, H. E. Bennett, A. H. Guenther, M. R. Kozlowski, B. E. Newnam, and M. J. Soileau, eds., Proc. SPIE **2428**, 435–443 (1995).
48. F. Bonneau, P. Combis, J. Vierne, and G. Daval, "Simulations of laser damage of SiO_2 induced by a spherical inclusion," in *Laser-Induced Damage in Optical Materials: 2000*, G. J. Exarhos, A. H. Guenther, M. R. Kozlowski, K. L. Lewis, and M. J. Soileau, eds., Proc. SPIE **4347**, 308–315 (2001).
49. H. C. van de Hulst, *Light Scattering by Small Particles* (Wiley, New York, 1957).
50. J. A. Stratton, *Electromagnetic Theory* (McGraw-Hill, New York, 1941).
51. W. J. Wiscombe, "Improved Mie scattering algorithms," Appl. Opt. **19**, 1505–1509 (1980).
52. F. P. Incropera and D. P. DeWitt, *Introduction to Heat Transfer* (Wiley, New York, 1996).